

C–C Reductive Elimination in Palladium Complexes, and the Role of Coupling Additives. A DFT Study Supported by Experiment

Martín Pérez-Rodríguez,[†] Ataulpa A. C. Braga,^{||} Max Garcia-Melchor,[‡] Mónica H. Pérez-Temprano,[§] Juan A. Casares,[§] Gregori Ujaque,[‡] Angel R. de Lera,[†] Rosana Álvarez,^{*,†} Feliu Maseras,^{*,‡,||} and Pablo Espinet^{*,§}

Departamento de Química Orgánica, Facultad de Química, Universidade de Vigo, Lagoas-Marcosende s/n, 36310 Vigo, Galicia, Spain, Institute of Chemical Research of Catalonia (ICIQ), Av. Països Catalans, 16, 43007 Tarragona, Catalonia, Spain, Unitat de Química Física, Edifici Cn, Universitat Autònoma de Barcelona, 08193 Bellaterra, Catalonia, Spain, and IUCINQUIMA/Química Inorgánica, Facultad de Ciencias, Universidad de Valladolid, 47071 Valladolid, Castilla y León, Spain

Received October 11, 2008; E-mail: rar@uvigo.es; fmaseras@iciq.es; espinet@qi.uva.es

Abstract: A DFT study of R–R reductive elimination (R = Me, Ph, vinyl) in plausible intermediates of Pd-catalyzed processes is reported. These include the square-planar tetracoordinated systems *cis*-[PdR₂(PMe₃)₂] themselves, possible intermediates *cis*-[PdR₂(PMe₃)L] formed in solution or upon addition of coupling promoters (L = acetonitrile, ethylene, maleic anhydride (ma)), and tricoordinated intermediates *cis*-[PdR₂(PMe₃)] (represented as L = empty). The activation energy ranges from 0.6 to 28.6 kcal/mol in the gas phase, increasing in the order vinyl–vinyl < Ph–Ph < Me–Me, depending on R, and ma < “empty” < ethylene < PMe₃ ≈ MeCN, depending on L. The effect of added olefins was studied for a series of olefins, providing the following order of activation energy: *p*-benzoquinone < ma < *trans*-1,2-dicyanoethylene < 3,5-dimethylcyclopent-1-ene < 2,5-dihydrofuran < ethylene < *trans*-2-butene. Comparison of the calculated energies with experimental data for the coupling of *cis*-[PdMe₂(PPh₃)₂] in the presence of additives (PPh₃, *p*-benzoquinone, ma, *trans*-1,2-dicyanoethylene, 2,5-dihydrofuran, and 1-hexene) reveals that: (1) There is no universal coupling mechanism. (2) The coupling mechanism calculated for *cis*-[PdMe₂(PMe₃)₂] is direct, but PPh₃ retards the coupling for *cis*-[PdMe₂(PPh₃)₂], and DFT calculations support a switch of the coupling mechanism to dissociative for PPh₃. (3) Additives that would provide intermediates with coupling activation energies higher than a dissociative mechanism (e.g., common olefins) produce no effect on coupling. (4) Olefins with electron-withdrawing substituents facilitate the coupling through *cis*-[PdMe₂(PR₃)(olefin)] intermediates with much lower activation energies than the starting complex or a tricoordinated intermediate. Practical consequences are discussed.

Introduction

The field of transition metal-catalyzed C–C and C–Het coupling processes^{1–3} has witnessed an explosion of empirical research aimed at the promotion of otherwise difficult reactions. Notable among those are the C–C coupling of aryl chlorides with a variety of organometallic partners (B, Sn, Mg, or Zn nucleophiles),^{4,5} and the formation of C–Het (N, O, S) bonds.^{6,7} Hartwig has nicely summarized the experimental results ac-

cumulated in the past decade or so and discussed the role of each partner (reactive ligands and ancillary ligands, electronic, and steric effects) on the coupling rate and efficiency.⁸ One interesting conclusion is that C–C and C–Het couplings can be discussed under very similar schemes. Novel bulky phosphines^{9,10} and carbene ligands¹¹ have been instrumental to facilitate these processes. The role of solvents and additives has been investigated.⁴ Kinetic analysis of the processes, isolation of reaction intermediates, monitoring of the evolution of these species,^{4,12,13} and computational studies^{14–17} have corroborated or modified mechanistic proposals, or suggested stimulating

[†] Universidade de Vigo.

^{||} ICIQ.

[‡] Universitat Autònoma de Barcelona.

[§] Universidad de Valladolid.

- (1) Brown, J. M.; Cooley, N. A. *Chem. Rev.* **1988**, *88*, 1031–1046.
- (2) Ozawa, F. Reductive Elimination. In *Fundamentals of Molecular Catalysis*; Kurosawa, H., Yamamoto, A., Eds.; Elsevier: New York, 2003; Vol. 3, pp 479–511.
- (3) (a) de Meijere, A.; Diederich, F.; *Metal Catalyzed Cross-Coupling Reactions*, 2nd ed.; John Wiley & Sons: New York, 2004. (b) Tamao, K.; Miyaura, N. *Cross-Coupling Reactions; Topics in Current Chemistry*; Springer: Berlin, 2002; Vol. 219. (c) Ziegler, T. *Chem. Rev.* **1991**, *91*, 651–667.

- (4) Espinet, P.; Echavarren, A. M. *Angew. Chem., Int. Ed.* **2004**, *43*, 4704–4734.

- (5) Littke, A. F.; Fu, G. C. *Angew. Chem., Int. Ed.* **2002**, *41*, 4177–4211.

- (6) Hartwig, J. F. *Acc. Chem. Res.* **1998**, *31*, 852–860.

- (7) Hartwig, J. F. *Angew. Chem., Int. Ed.* **1998**, *37*, 2046–2067.

- (8) Hartwig, J. F. *Inorg. Chem.* **2007**, *46*, 1936–1947.

- (9) Littke, A. F.; Fu, G. C. *Angew. Chem., Int. Ed.* **1998**, *37*, 3387–3388.

- (10) Barder, T. E.; Walker, S. D.; Martinelli, J. R.; Buchwald, S. L. *J. Am. Chem. Soc.* **2005**, *127*, 4685–4696.

- (11) Herrmann, W. A. *Angew. Chem., Int. Ed.* **2002**, *41*, 1290–1309.

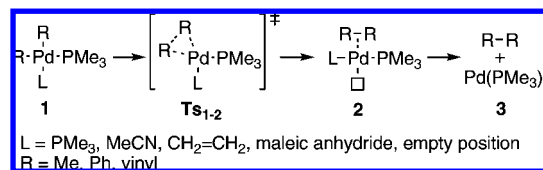
alternative mechanistic views. Nowadays, the excessively schematic mechanisms of metal-catalyzed cross-coupling reactions are being revisited, and more detailed and complex views are replacing the traditional beliefs.

Recent results show that each of the main steps in the catalytic cycle of Pd-catalyzed coupling reactions (oxidative addition, transmetalation, isomerization, and reductive elimination) can be rate determining, depending on the reagents, the ligands, the solvent, and the additives.⁴ Often taken for granted, the final C–C or C–Het coupling is critical for the success of the reaction, as the other steps are frequently reversible,¹³ and it is the irreversible reductive elimination that must pull the catalytic cycle forward. Since the early theoretical works of Tatsumi, Hoffmann, Yamamoto and Stille,¹⁸ and Low and Goddard,¹⁹ the reductive elimination step had received scant attention, but recently Ananikov, Musaev, and Morokuma carried out extensive studies on the C–C reductive elimination, in the gas phase, of the most common types of coupling partners in square-planar *cis*-[MRR'(PH₃)₂] complexes (R or R' = methyl, vinyl, phenyl, alkynyl; M = Pd, Pt).²⁰ Moreover, Bo et al. studied the effect of the bite angle of chelating diphosphines on the formation of C–C and C–O bonds.²¹ The feasibility of Ar–F elimination from Pd(II) has been theoretically assessed and then experimentally addressed.²² Finally, during the development of the present study, Ananikov, Musaev, and Morokuma published a theoretical investigation of the reductive elimination from square planar and T-shaped Pd species with phosphines of different bulkiness.²³ Despite these recent contributions, the theoretical description of the reductive elimination step is still rather incomplete. For instance, the role of additives, solvents, or other ligands present in solution is not well understood, and the feasibility under experimental circumstances of the species proposed *in-silico* has not been experimentally tested. This article reports theoretical results on *cis*-[PdMe₂(PMe₃)L] systems that model some C–C coupling conditions, which are then compared to experimental results on *cis*-[PdMe₂(PPh₃)₂] + L systems.

Computational Models

The models chosen, *cis*-[PdRR'(PMe₃)L] (R = Me, vinyl, and Ph) complexes, represent, depending on L, plausible coupling

Scheme 1



intermediates formed in the presence of solvents, ligands, or coupling additives. The ancillary ligand PMe₃ was chosen as a more realistic phosphine model than PH₃. Nonsymmetrical complexes (PdRR'L₂) were spared because it has been shown that their computed activation energies are roughly the average between those of their symmetrical counterparts;²⁰ note, however, that experimental evidence shows that coupling rates are faster for PdRR'L₂ than for PdR₂L₂ or PdR'L₂.⁸ The following L ligands were used: (i) L = PMe₃ gives square-planar tetracoordinated complexes *cis*-[MR₂(PMe₃)₂]; (ii) L = MeCN models σ -donor coordinating solvents of moderate donating ability; (iii) L = ethylene represents π -coordinating molecules present in solution in cross-coupling reactions involving vinyl, allyl, and other C=C containing moieties,²⁴ for example, the starting electrophile or the coupling product; (iv) L = ma (maleic anhydride, an electron-withdrawing olefin) was included due to reports showing that electron-withdrawing olefins are additives that promote the reductive elimination step;²⁵ and (v) finally, L = "empty position" represents tricoordinated T-shaped *cis*-[PdR₂(PR₃)] complexes with only one ancillary phosphine ligand, suggested by kinetic studies to be coupling intermediates in some cases.^{10,18,26} Evidence for the formation of monophosphine complexes with one bulky phosphine as the only ancillary ligand includes crystal structures of apparently tricoordinated complexes, in which Pd turns out to be stabilized by weak agostic interactions,^{27,28} and also true T-shaped complexes.²⁸ A theoretical study of the factors making T-shaped palladium complexes more accessible has appeared very recently.²⁹

As this work was progressing, the experimental tests in parallel to the initial calculations pushed us to extend the models to gain insight on the effect of olefins. On the other hand, a study dealing with case (v) appeared, which covered some aspects pursued in this chapter of our study.²³ Our data on case (v) are still needed in the context of our discussion, but, for the sake of page economy, only the novel aspects of tricoordinated intermediates will be dealt with in the text, while more information is given in the Supporting Information.

Results and Discussion

Overall Reaction Profile. The reductive elimination process shows four significant stages in the reaction profile (Scheme 1):^{19–21,23} (i) the *cis* reactant species, **1**; (ii) the transition state TS_{1–2}; (iii) an intermediate adduct, **2**, with the R–R coupling product weakly bound to the metal center; and (iv) the coupling product already separated from the Pd(0) complex (stage **3**). Each stage was computed for all R and L combinations (R =

- (12) Casares, J. A.; Espinet, P.; Fuentes, B.; Salas, G. *J. Am. Chem. Soc.* **2007**, *129*, 3508–3509.
- (13) Pérez-Temprano, M. H.; Nova, A.; Casares, J. A.; Espinet, P. *J. Am. Chem. Soc.* **2008**, *130*, 10518–10520.
- (14) Niu, S.; Hall, M. B. *Chem. Rev.* **2000**, *100*, 353–405.
- (15) Goossen, L. J.; Koley, D.; Hermann, H. L.; Thiel, W. *J. Am. Chem. Soc.* **2005**, *127*, 11102–11114.
- (16) (a) Braga, A. A. C.; Morgon, N. H.; Ujaque, G.; Maseras, F. *J. Am. Chem. Soc.* **2005**, *127*, 9298–9307. (b) Nova, A.; Ujaque, G.; Maseras, F.; Lledós, A.; Espinet, P. *J. Am. Chem. Soc.* **2006**, *128*, 14571–14578. (c) Braga, A. A. C.; Ujaque, G.; Maseras, F. *Organometallics* **2006**, *25*, 3647–3658.
- (17) (a) Alvarez, R.; Faza, O. N.; López, C. S.; de Lera, A. R. *Org. Lett.* **2006**, *8*, 35–38. (b) Alvarez, R.; Faza, O. N.; de Lera, A. R.; Cárdenas, D. J. *Adv. Synth. Catal.* **2007**, *349*, 887. (c) Alvarez, R.; Pérez, M.; Faza, O. N.; de Lera, A. R. *Organometallics* **2008**, *27*, 3378–3389.
- (18) Tatsumi, K.; Hoffmann, R.; Yamamoto, A.; Stille, J. K. *Bull. Chem. Soc. Jpn.* **1981**, *54*, 1857–1867.
- (19) (a) Low, J. J.; Goddard, W. A. *Organometallics* **1986**, *5*, 609–622. (b) Low, J. J.; Goddard, W. A. *J. Am. Chem. Soc.* **1986**, *108*, 6115–6128.
- (20) Ananikov, V. P.; Musaev, D. G.; Morokuma, K. *Organometallics* **2005**, *24*, 715–723.
- (21) Zuidema, E.; Van Leeuwen, P. W. N. M.; Bo, C. *Organometallics* **2005**, *24*, 3703–3710.
- (22) Yandulov, D. V.; Tran, N. T. *J. Am. Chem. Soc.* **2007**, *129*, 1342–1358.
- (23) Ananikov, V. P.; Musaev, D. G.; Morokuma, K. *Eur. J. Inorg. Chem.* **2007**, 5390–5399.

- (24) Albéniz, A. C.; Espinet, P.; Martín-Ruiz, B. *Chem.-Eur. J.* **2001**, *7*, 2481–2489.
- (25) (a) Goliaszewski, A.; Schwartz, J. *J. Am. Chem. Soc.* **1984**, *106*, 5028–5030. (b) Goliaszewski, A.; Schwartz, J. *Tetrahedron Lett.* **1985**, *26*, 5779–5789. (c) Kluwer, A. M.; Elsevier, C. J.; Bühl, M.; Lutz, M.; Spek, A. L. *Angew. Chem., Int. Ed.* **2003**, *42*, 3501–3504. (d) Sustmann, R.; Lau, J. *Chem. Ber.* **1986**, *119*, 2531–2541.
- (26) Louie, J.; Hartwig, J. F. *J. Am. Chem. Soc.* **1995**, *117*, 11598–11599.
- (27) (a) Stambuli, J. P.; Bühl, M.; Hartwig, J. F. *J. Am. Chem. Soc.* **2002**, *124*, 9346–9347. (b) Stambuli, J. P.; Incarvito, C. D.; Bühl, M.; Hartwig, J. F. *J. Am. Chem. Soc.* **2004**, *126*, 1184–1194.
- (28) Yamashita, M.; Hartwig, J. F. *J. Am. Chem. Soc.* **2004**, *126*, 5344–5345.
- (29) Moncho, S.; Ujaque, G.; Lledós, A.; Espinet, P. *Chem.-Eur. J.* **2008**, *14*, 8986–8994.

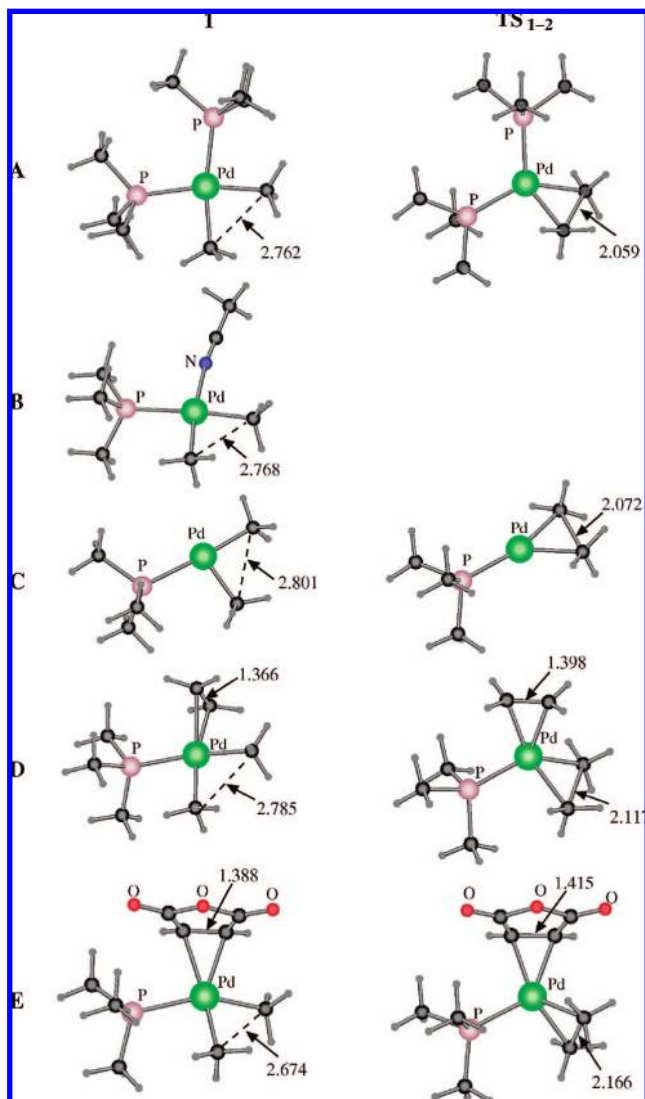


Figure 1. Optimized geometry of the reactant **1** and the transition state **TS**₁₋₂ for the reductive elimination of ethane. (A) L = PMe₃; (B) L = MeCN; (C) L = empty; (D) L = CH₂CH₂; (E) L = ma. Relevant selected distances (Å) are shown.

Me, Ph, vinyl; L = empty position, ethylene, PMe₃, ma, MeCN). Details of the 60 computed geometries, tables of selected geometrical parameters, and a discussion of the geometrical changes along the reductive elimination are given as Supporting Information.

The structures of the reactants and the transition states are shown in Figure 1 for R = Me (for the other R groups the coordination geometries are similar). Fairly symmetrical concomitant shortening of the C–C distance and elongation of the Pd–C distances is observed as the reactants evolve to their transition states. For L = empty, the coupling is direct. For L ≠ empty, the calculation predicts also direct coupling, now in the tricoordinated complex. As an exception (not found in any of the published studies), for R = Me and L = MeCN a stepwise mechanism is predicted, initiated by MeCN dissociation and followed by coupling in the resulting tricoordinated complex. It makes sense that the case of a dissociative coupling is found in the calculation for the combination of the strongest R σ-donor (Me) with MeCN, which is a weak donor, non π-acceptor ligand.

Influence of the R Group on the Energy Barrier. Table 1 gathers ΔG[‡] data calculated for the 15 reductive eliminations

Table 1. Thermodynamic Data (ΔG[‡] in kcal/mol, Relative to Reactant **1**) for the Reductive Elimination of R–R Starting from the *cis*-[PdR₂(PMe₃)(L)] Complexes

R	L	TS ₁₋₂ ^a	2 ^a	3 ^a
Me	ma	8.6	–43.0	–49.3
	empty	13.2	–19.9	–25.6
	CH ₂ CH ₂	21.7	–34.8	–43.7
	MeCN	27.0 ^b	–32.9	–37.8
	PMe ₃	28.6	–35.0	–43.1
Ph	ma	2.9	–46.4	–50.7
	empty	4.9	–33.3	–27.2
	CH ₂ CH ₂	11.3	–30.9	–43.7
	MeCN	13.2	–31.2	–36.1
	PMe ₃	12.8	–33.9	–41.9
vinyl	ma	0.6	–56.2	–51.9
	empty	4.9	–39.9	–24.9
	CH ₂ CH ₂	8.9	–43.0	–43.3
	MeCN	11.9	–32.6	–35.6
	PMe ₃	11.5	–36.1	–40.1

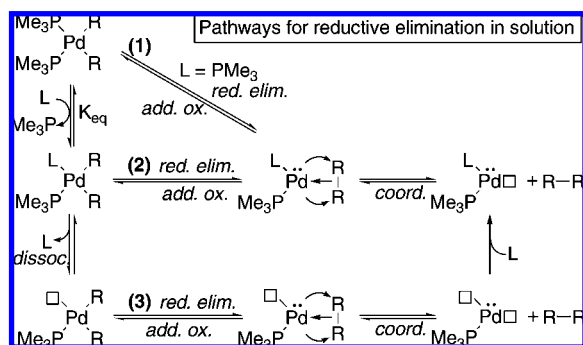
^a In gas phase. Values in acetonitrile including solvation energies using a continuum model are given in the Supporting Information.

^b This value corresponds to the overall energy barrier for the stepwise mechanism (see text).

from *cis*-[PdR₂(PMe₃)L]. The trend of computed barriers is Csp³–Csp³ > C_{Ar}–C_{Ar} > Csp²–Csp² for any series with an identical L ligand (occasional exceptions within the error of calculation are found for very similar values of C_{Ar}–C_{Ar} and Csp²–Csp² data). This and the trends in bond angles and lengths (Supporting Information) are in coincidence with the sequences reported for *cis*-[PdR₂(PH₃)₂] complexes.²⁰

In general, the structures where Me–Me elimination occurs deviate from planarity, and the corresponding transition states **TS**₁₋₂ show distorted tetrahedral structures around the metal. In contrast, the complexes with Ph or vinyl groups feature almost planar **TS**₁₋₂ structures. The higher directionality of the M–C(sp³) bond, its weaker M–C bond dissociation energy, and a larger influence of steric effects have been deemed responsible for these structural differences.²⁰ Whereas the activation energies reported for PH₃ complexes are about 4 times lower for the Csp²–Csp² relative to the Csp³–Csp³ bond formation,²⁰ the differences calculated for the bulkier PMe₃ ligand are significantly smaller (2.5-fold at most). This could be due to a destabilization of the reactants **1** for R = Me, arising from the higher crowding with PMe₃ as compared to PH₃, which could attenuate the differences in energy for higher absolute values. All of the coupling processes are strongly exothermic, which makes the C–C coupling irreversible. Values differing by as much as 25 kcal/mol are computed for eliminations starting from tricoordinated Pd versus tetracoordinated Pd complexes. For the latter, the more exothermic reductive eliminations for each R are those with ma as auxiliary ligand, followed by those with ethylene, phosphine, and acetonitrile. The significance of these thermodynamic results should not be overemphasized, however, as its connection to the experimental conditions is not straightforward. Considering, for instance, a catalytic process in the presence of excess PMe₃ as auxiliary ligand and with ma as coupling promoter, the most likely Pd(II) species in solution preceding the coupling will be [PdR₂(PMe₃)₂], in equilibrium with minute amounts of a [PdR₂(PMe₃)(ma)] intermediate, due to the fact that PMe₃ is a much better ligand toward Pd(II) than is ma. On the other hand, coordination of the strongly acceptor ma is much better in the

Scheme 2



reduced Pd(0) complex $[\text{Pd}(\text{PMe}_3)_2(\text{ma})]$.³⁰ Consequently, the thermodynamic balance for the experimental reductive elimination might well correspond to a process going from $\text{PdR}_2(\text{PMe}_3)_2 + \text{ma}$ to $\text{Pd}(\text{PMe}_3)_2(\text{ma}) + \text{R}-\text{R}$, rather than any of the direct coupling models studied here.

The activation barriers calculated are much higher for $\text{R} = \text{Me}$ than for $\text{R} = \text{Ph}$ or vinyl, both in vacuum and in continuum MeCN solution. The values for the coupling of Csp^3 centers are so high in some cases (e.g., ca. 28.6 kcal/mol when $\text{L} = \text{PMe}_3$) that this step becomes a likely candidate to be rate determining in a cycle. In other words, failures in coupling alkyl organometallics with alkyl halides or pseudohalides should not be attributed cursorily to the oxidative addition or the transmetalation step. For $\text{R} = \text{Ph}$ and vinyl, the activation barriers are smaller and likely less critical for synthetic purposes. It is worth mentioning that a continuum solvent correction (see Supporting Information) increases more the calculated barriers for $\text{R} = \text{vinyl}$, making vinyl and phenyl barriers similar.

Very interestingly, Table 1 reveals that the influence of R is not necessarily prevailing over other factors, and can be overcome if different L ligands are used to couple different R groups (i.e., $\text{cis}-[\text{PdR}_2(\text{PMe}_3)\text{L}]$ versus $\text{cis}-[\text{PdR}'_2(\text{PMe}_3)\text{L}']$). In other words, the nature of L is extremely important.

Influence of the L Group on the Coupling Barrier. This factor has not been theoretically considered in the literature. In an experimental reaction using phosphines as the initial ligands, the model complexes studied here could be interconnected by ligand-substitution or ligand-dissociation equilibria (Scheme 2).³¹ The reductive elimination would take place from tetracoordinated (pathways 1 and 2) or tricoordinated (pathway 3) complexes and should be the microscopic reverse of the oxidative addition of a nonpolar C–C bond. The latter is believed to follow a concerted mechanism,² where the oxidative

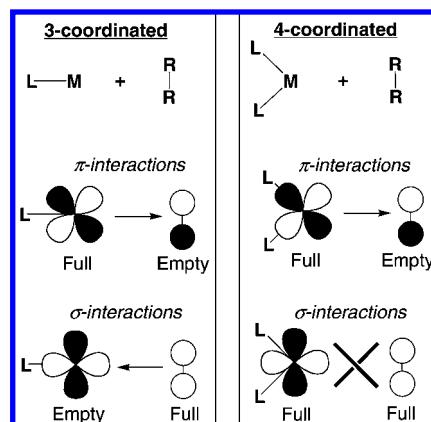


Figure 2. Key orbital interactions in the transition state for reductive elimination from tricoordinated complexes (left) and tetracoordinated complexes (right).

addition is the result of a side-on coordination of the single bond to the metal; σ -donation from the $\text{R}-\text{R}$ σ bonding orbital plus back-donation from the metal to the $\text{R}-\text{R}$ σ^* antibonding orbital will eventually break the $\text{R}-\text{R}$ bond. In fact, the geometries observed for the transition states TS_{1-2} , which are very symmetric for $\text{R} = \text{phenyl}$ and vinyl, and less so but still fairly symmetric for $\text{R} = \text{Me}$, support this mechanism.

The TS_{1-2} values in Table 1 indicate that, for each R group considered, the activation energy for different L ligands decreases in the order $\text{MeCN} \approx \text{PMe}_3 > \text{CH}_2\text{CH}_2 > \text{“empty”} > \text{ma}$. The range of energy values is large, and larger for the complexes with $\text{R} = \text{Me}$ reflecting the higher absolute values involved in the reductive elimination of this group. Synthetic interest is usually to favor the coupling, and we will discuss in the following sections the reasons why the cases of $\text{L} = \text{empty}$ and $\text{L} = \text{ma}$ are particularly favorable.

The geometry of the $\text{C}-\text{Pd}-\text{C}$ triangle is relatively similar for all of the computed tetracoordinated transition states, but the reductive elimination from tricoordinated complexes (the case $\text{L} = \text{empty}$) is different from the others, as this is the only case where the bond is formed in a position trans to the phosphine ligand (Figure 1). The qualitative difference in reductive elimination from tetracoordinated or from tricoordinated complexes has been previously noted and analyzed using simple extended Hückel descriptions,^{18,32} and by DFT calculations in a recent study.²³ Those computational studies and ours show that the reductive elimination is easier for the tricoordinated systems. This lower reductive elimination barrier in tricoordinated systems ($\text{L} = \text{“empty”}$) can be explained considering the orbital interactions shown in Figure 2. The key factor is the different occupation of the σ_{M} orbital for 3-coordinated and 4-coordinated d^8 complexes in the corresponding symmetry.³³ Whereas for both types of complex the interactions roughly corresponding to π -symmetry are bonding, those roughly corresponding to σ -symmetry are repulsive for the two interacting full orbitals in the 4-coordinated system, but bonding for the empty–full interaction in the 3-coordinated system. This orbital diagram also explains the fact that the forming C–C bond is placed trans to the phosphine in the tricoordinated system. It follows as well from this diagram that any external

(30) Espinet, P.; Albéniz, A. C. In *Comprehensive Organometallic Chemistry*; Mingos, D. M. P., Crabtree, R. H., Canty, A., Eds.; Elsevier: Oxford, 2007; Vol. 8, pp 317–332.

(31) In principle, these equilibria could be analyzed theoretically from the computed ligand dissociation energies, collected in Table S14 of the Supporting Information, but estimation of these specific equilibrium constants with the computational methods applied is troublesome. In fact, the two magnitudes reported, potential energy and free energy, present sharply different values, with differences around 16 kcal/mol. This discrepancy proves the importance of entropic corrections in these bimolecular processes. Unfortunately, in our computational approach, these particular terms are estimated through assumption of ideal gas behavior of the molecules, which is obviously not the optimal choice for systems in solution. Moreover, experimental reactions can be carried out in solvents of very different polarity. Thus, rather than focusing on the intrinsically inaccurate estimation of these equilibrium constants, we decided to analyze the trends in the computed activation barriers associated with the different ligands, where entropic contributions are less critical.

(32) Tatsumi, K.; Nakamura, A.; Komiya, S.; Yamamoto, A.; Yamamoto, T. *J. Am. Chem. Soc.* **1984**, *106*, 8181–8188.

(33) Jean, Y. *Molecular Orbitals of Transition Metal Complexes*; Oxford University Press: London, 2005.

factor withdrawing density from the σ_M orbital in a 4-coordinated molecule will lower the barrier for reductive elimination in tetracoordinated compounds.

The low barrier associated with the tricoordinated system has important mechanistic implications. If there is a weak ligand, or if the crowding in the tetracoordinated complex is high, tricoordination will be more easily accessible,²⁹ and it may be energetically more efficient for the system to release one ligand and undergo reductive elimination from the tricoordinated species (pathway 3 in Scheme 2). In fact, this is what we find in our calculations for *cis*-[PdMe₂(PMe₃)(NCMe)], and in our experiments for *cis*-[PdMe₂(PPh₃)₂] (see later). Dissociative coupling might be fairly general for reasonably hindered compounds.

For the cases found to couple directly in *cis*-[PdMe₂(PMe₃)L], the trend PMe₃ > CH₂CH₂ > ma confirms that the barrier decreases with the π -acceptor ability of L. As discussed above, the more π -acceptor the ligand, the lower should be the coupling barrier because they draw electron density away from the σ_M and this orbital is antibonding in the transition state. Consistently, ethylene is a better π -acceptor than is PMe₃ and produces a lower coupling barrier. The barrier for ma is even lower because it is a much stronger π -acceptor,^{34,35} to the point that the coupling is calculated to be easier for the tetracoordinated complex with ma than for the tricoordinated species (for R = Me, ΔG^\ddagger is 21.7 for L = ethylene, 13.2 kcal/mol for the tricoordinated species, and 8.6 kcal/mol for L = ma).

Electronic and Structural Factors in Olefins. The structures of the reactant **1** and the transition state TS₁₋₂, for ethylene and ma (Figure 1), show that for ethylene the olefin rotates from a perpendicular to an “in-plane” coordination during the reaction, whereas ma is coordinated in-plane already in the reactant. The olefin orientation is defined by the Pd–P–X–C_{olefin} dihedral angle, where X is the midpoint of the C=C bond. In the reactant, the dihedral angle is 89.0° for ethylene, but only 9.0° for MA. In the transition state, however, the double bond is practically in the metal plane in both cases (dihedral values of 0.1° for CH₂CH₂, and 6.5° for ma). To examine this matter, additional systems with the ligands *trans*-2-butene, fumaronitrile (*trans*-1,2-dicyanoethylene), 3,5-dimethylcyclopent-1-ene, and 2,5-dihydrofuran were studied. Fumaronitrile was chosen as a strong π -accepting olefin with no hindrance to perpendicular coordination; 3,5-dimethylcyclopent-1-ene is a conjugated cyclic olefin with expectedly medium π -acceptor properties; 2,5-dihydrofuran is a cyclic olefin structurally very similar to ma, but without electron-withdrawing substituents; and *trans*-2-butene is sterically similar to *trans*-1,2-dicyanoethylene, but lacks strong electron-withdrawing substituents. Only the reactant and the transition state with R = Me were computed for these systems. The key results are summarized in Figure 3 for the geometries, and in Table 2 for the computed energy barriers.

The computed geometries show that, for the transition state, the torsion angle is always close to 0°, regardless of the structure aspect of the olefin. The in-plane arrangement observed for TS₁₋₂ is also observed in the final Pd(0) product (stage **3**) and

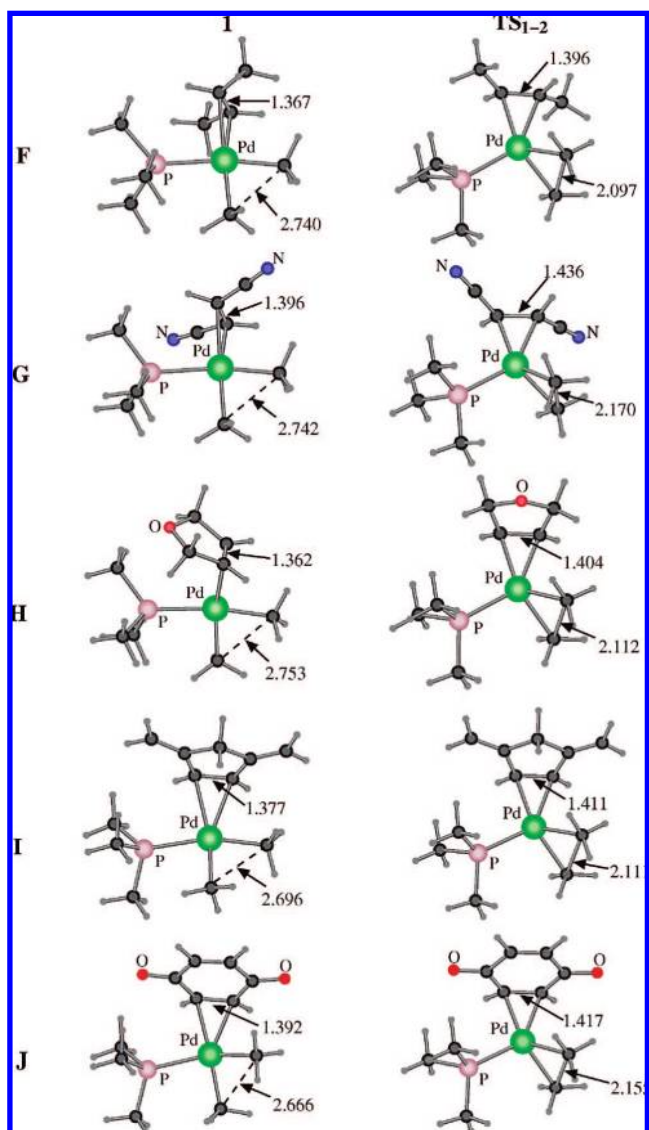


Figure 3. Optimized geometry of the reactant **1** and the transition state TS₁₋₂ for additional olefins with different steric and electronic features. (F) L = *trans*-2-butene; (G) L = *trans*-1,2-dicyanoethylene; (H) 2,5-dihydrofuran; (I) L = 3,5-dimethylcyclopent-1-ene; (J) L = *p*-benzoquinone. Relevant selected distances (in Å) are shown.

Table 2. Computed Energy Barrier (ΔG^\ddagger , kcal/mol) and Orientation (deg) of Olefin for the Reductive Elimination of Me–Me Starting from the *cis*-[PdMe₂(PMe₃)(L)] Complexes

entry	L	ΔG^\ddagger	P–Pd–X–C _{olefin} (1)	P–Pd–X–C _{olefin} (TS ₁₋₂)
1	<i>trans</i> -2-butene	23.0	65.1	4.2
2	ethylene	21.7	89.0	0.1
3	2,5-dihydrofuran	19.8	88.3	−0.4
4	3,5-dimethylcyclopent-1-ene	15.9	13.5	−0.4
5	<i>trans</i> -1,2-dicyanoethylene	10.0	71.7	6.0
6	maleic anhydride	8.6	9.0	6.5
7	<i>p</i> -benzoquinone	5.9	10.9	−2.4
8	empty	13.2		

in the structures found experimentally for [PdL₂(olefin)] complexes.³⁰ Along with an incipient Me–Me bond (compare C–C distances of about 2.8 Å in the Pd(II) reactants **1** with 2.1–2.2 Å in TS₁₋₂ and 1.54 Å for a C–C single bond), the transition states show a clear elongation (about 0.03–0.04 Å) of the coordinated C=C double bond, reflecting the increased electron

(34) Albéniz, A. C.; Espinet, P.; Pérez-Mateo, A.; Nova, A.; Ujaque, G. *Organometallics* **2006**, *25*, 1293–1297.

(35) The ma ligand is a very strong π -acceptor, to the point that the oxidation level of its formally Pd(0) complexes must be relatively high. This is shown, for instance, by the fact that these complexes are air stable and difficult to oxidize (see refs 30 and 33). It looks reasonable that, as the reductive elimination progresses, the overall π -acceptance will increase more steeply for ma than for other poorer π -acceptors, making this lowering of the barrier particularly effective.

back-donation to the olefin π^* orbitals. This supports the qualitative orbital diagram proposed in Figure 2, which predicts strong electronic preference for the in-plane arrangement in TS_{1-2} .

There is no general preferred arrangement of the olefin for the reactants **1**. Angles spanning the whole range $0-90^\circ$ are found, apparently not related to the π -acceptor strength of the olefin. Typically, simple olefins coordinate to Pd(II) with the double bond roughly perpendicular to the coordination plane (entry 2), or making a somewhat smaller angle to minimize interligand repulsion (entries 1 and 5). It would appear that for cyclic-planar olefins the in-plane coordination is favored (entries 4, 6, and 7), but this is not the case of 2,5-dihydrofuran (entry 3). Inspection of the calculated structures suggests that often there are only minor differences (1–3 kcal/mol) for alternative arrangements and in many cases the minimum might be dictated by subtle steric repulsions. Hence, although one could wonder whether the in-plane coordination of the double bond “prepares” the reactant for reductive elimination, in fact there is no conclusive support for this (nor against) in Table 2.³⁶

There is, however, a clear relationship with the electronic effect of the olefin substituents. Comparing for instance entries 1, 2, and 5, the substituents have only a small effect on the structure, which should hardly affect the energy barrier, and the sequence of ΔG^\ddagger observed (*trans*-2-butene > CH_2CH_2 > *trans*-1,2-dicyanoethylene) corresponds to the increase of electron withdrawal (or decrease of electron donation) of the substituents. This electronic effect is expected to be smaller for the reactant, where the π back-donation ability of Pd(II) is modest,³⁷ than for the transition state, which is very much stabilized by electron withdrawal from the antibonding orbital σ_{M} (Figure 2). Replacement of H by Me (entry 1 vs 2) brings about only a minor increase in activation barrier of 1.3 kcal/mol, while the inclusion of strong π -acceptor substituents ($\text{C}\equiv\text{N}$ or $\text{C}=\text{O}$) produces a substantial lowering of the barrier. The differences of 13 kcal/mol between *trans*-2-butene and fumaronitrile (entries 1 and 5), and 11.2 kcal/mol between 2,5-dihydrofuran and maleic anhydride (entries 3 and 6), clearly reflect the enormous importance of the π -acceptor ability of L on the reductive elimination process. Dimethylcyclopent-1-ene (entry 4), a less strong acceptor olefin, produces intermediate values. The optimal effects are achieved for maleic anhydride and *p*-benzoquinone (entries 6 and 7), which appear very good choices as coupling additives. Very interestingly, these and the fumaronitrile (entries 5–7) provide a lower coupling barrier on the tetracoordinated complex than the barrier for the tricoordinated (entry 8).

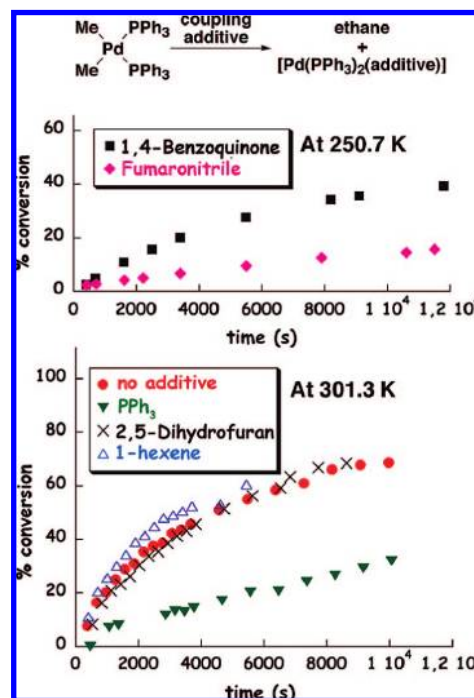


Figure 4. Coupling conversion of $[\text{PdMe}_2(\text{PPh}_3)_2]$ (**4**) in acetone- d_6 in the presence of additives. Upper plot is at 250.7 K, for the fast reactions; for the rest, no conversion is observed at this temperature. Lower plot is at 301.3 K, for the fast reactions; the conversion for fumaronitrile or *p*-benzoquinone at this temperature is 100% in the first measurement and is not plotted.

Experimental Studies on the System *cis*- $[\text{PdMe}_2(\text{PPh}_3)_2]$ + Additive. The computational results above indicate clearly which features in L should favor the reductive elimination in complexes *cis*- $[\text{PdR}_2(\text{PR}'_3)_2]$. It is difficult, however, to find in the literature quantitative experimental support for these predictions, as in operational catalytic systems the *cis*- $[\text{PdR}_2(\text{PR}'_3)_2]$ intermediates should be non observable. We decided to study the systems *cis*- $[\text{PdMe}_2(\text{PPh}_3)_2]$ (**4**) + additive (additive = PPh_3 , *ma*, *p*-benzoquinone, fumaronitrile, dihydrofuran, 1-hexene) in acetone- d_6 .³⁸ Three circumstances in the real system differ from the theoretical conditions. First, the experimental phosphine used is somewhat bulkier and less basic. Second, in the experimental system, the corresponding complexes **1**, where the calculation starts, must be formed in solution (except for L = PPh_3) by dissociation (for L = empty) or by ligand substitution (Scheme 2), which means that not only the TS_{1-2} but also the preequilibrium constant that determines the concentration of **1** will influence the coupling rate observed. Finally, the experimental reactions are studied in acetone- d_6 , which is a hard coordinating solvent. In other words, the experimental study deals with a related but not identical process, shown on top of Figure 4.

The experiments with maleic anhydride revealed the formation of ethane and methane, the latter associated with Pd–Me acidolysis by maleic acid produced by the water contamination of the acetone- d_6 (Scheme 3). At low temperature, the formation of the corresponding Pd(0) and Pd(II) products was confirmed. Thus, although *ma* induces very fast coupling (comparable to

- (36) An additional set of calculations we carried out to check whether the energy barrier to olefin rotation could be relevant to the overall kinetics. In these calculations, collected in the Supporting Information (Figure S15), we found two local minima for *cis*- $[\text{PdMe}_2(\text{PMe}_3)(\text{H}_2\text{C}=\text{CH}_2)]$. The most stable one is the out-of-plane species reported in the text; a secondary in-plane species is 4.7 kcal/mol higher in energy. The transition state between these two minima is only 1.2 kcal/mol above the least stable minimum, indicative of a fast process at room temperature.
- (37) The filled d orbitals in square-planar Pd(II) complexes are very stable, and this reduces their involvement in back donation. This can be noted, for instance, in the fact that Pd(II)–carbene bonds show typical single bond distances. See some X-ray structures in: (a) Albéniz, A. C.; Espinet, P.; Manrique, R.; Pérez-Mateo, A. *Angew. Chem., Int. Ed.* **2002**, *41*, 2363–2366. (b) Albéniz, A. C.; Espinet, P.; Manrique, R.; Pérez-Mateo, A. *Chem.-Eur. J.* **2005**, *11*, 1565–1573. (c) Albéniz, A. C.; Espinet, P.; Pérez-Mateo, A. *Organometallics* **2006**, *25*, 1293–1297.

- (38) PPh_3 was used instead of the PMe_3 used for calculations, due to its much easier handling. The choice turned out to be fortunate, and PPh_3 produced a range of coupling rates that could be monitored by ^1H NMR. Moreover, it contributed to reveal the importance of the steric effect of the phosphine.

Scheme 3

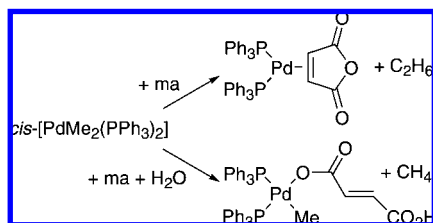


Table 3. Experiments at ca. 300 K

additive	concentration/ 10^{-3} mmol	temperature/K	$[4]_0/10^{-3}$ mmol
none		301.6	1.06
PPh ₃	1.02	301.6	1.06
fumaronitrile	3.28	301.0	1.06
<i>p</i> -benzoquinone	3.40	301.3	1.06
maleic anhydride	3.12	301.3	1.06
2,5-dihydrofuran	3.10	301.3	1.06
1-hexene	3.12	301.1	1.06

Table 4. Experiments at ca. 250 K

additive	concentration/ 10^{-3} mmol	temperature/K	$[4]_0/10^{-4}$ mmol
fumaronitrile	3.14	250.7	5.90
<i>p</i> -benzoquinone	3.09	250.7	5.90
maleic anhydride	3.11	250.7	5.90

p-benzoquinone), the actual rate could not be properly quantified. In a practical sense, ma looks to be a problematic coupling additive in reactions where complete dryness cannot be guaranteed.

For the other additives, the experimental results show a clear division. The strongly π -acceptor olefins produce a dramatic acceleration of the coupling, somewhat larger for the cyclic olefin *p*-benzoquinone. The common olefins do not produce any significant effect (the differences are within experimental error) on the coupling rate shown by *cis*-[PdMe₂(PPh₃)₂] alone. Finally, the addition of PPh₃ brings about retardation of the coupling, which is an indication of prior dissociation of phosphine before coupling takes place on a tricoordinated complex. This latter result is in contrast with our calculation for *cis*-[PdMe₂(PMe₃)₂], where coupling occurs in the tetracoordinated complex. Hence, the electronic and steric differences between PPh₃ and PMe₃ turn out to be mechanistically decisive, as dissociation becomes more accessible for the bulkier phosphine. In fact, DFT calculations for the dissociation process of *cis*-[PdMe₂(PR₃)₂] into *cis*-[PdMe₂(PR₃)] and PR₃ afford markedly different values: ΔE 12.1 kcal mol for R = Ph, versus 21.7 kcal mol for R = Me, which makes a considerable difference of 9.6 kcal mol, and clearly supports easier dissociation for R = Ph.³⁹ The entropic contributions, difficult to compute accurately, would further weigh in favor of a dissociative mechanism.⁴⁰ Experimental retardation of coupling had been reported for *cis*-

[PdMe₂(PPh₂Me)₂] upon addition of PPh₂Me,^{18,41} in DMF or THF, whereas coupling in tetracoordinated complexes was calculated for complexes with PH₃.²⁰ On the other hand, a dissociative mechanism was calculated here for *cis*-[PdMe₂(PMe₃)(NCMe)]. Thus, the interpretation of the rest of our calculated (with PMe₃) and experimental (with PPh₃) data has to be made in the light of this propensity to dissociation observed for the complexes with bulkier phosphines or with weaker L ligands.

Whereas the values in Table 2 predict a graduation of coupling activation energy from *cis*-[PdMe₂(PMe₃)(olefin)] for common olefins (entries 1–3), the experiments show no difference for the coupling of *cis*-[PdMe₂(PPh₃)₂] upon addition of olefin, whether linear (1-hexene) or cyclic (dihydrofuran). In these cases, the formation of small amounts in equilibrium of a putative *cis*-[PdMe₂(PPh₃)(olefin)] is kinetically insignificant,⁴² and the coupling occurs via dissociation to the tricoordinated [PdMe₂(PPh₃)] (path 3 in Scheme 2). As the replacement of PMe₃ by an olefin is even less favorable than that of PPh₃, it can be extrapolated that the addition of common olefins to promote the coupling in *cis*-[PdMe₂(PMe₃)₂] should also be ineffective, regardless of the theoretical prediction that a *cis*-[PdMe₂(PMe₃)(olefin)] intermediate would couple more easily than *cis*-[PdMe₂(PMe₃)₂], because that intermediate is not expected to form in kinetically significant amounts.

In contrast, the dramatic activating effect observed experimentally for π -acceptor olefins (Figure 4) indicates that, in these cases of considerably lower coupling barrier, the formation of a small proportion of intermediate *cis*-[PdMe₂(PPh₃)(acceptor olefin)] becomes kinetically decisive, and these olefins drive the reaction through pathway 2 in Scheme 2. In this respect, it is interesting to note that the recent use of chelating ligands providing P and electron-deficient olefin coordinating ends, P(acceptor olefin)R₂, has led to a dramatic improvement in efficiency of C(sp³)–C(sp³) and C(sp³)–C(sp²) couplings in Suzuki and Negishi reactions.⁴³ Obviously, the chelate effect helps to increase the stability and concentration of a coupling active intermediate *cis*-[PdR'R''(P(acceptor olefin)R₂)], and likely that of the corresponding transition state.

Conclusions

The C–C coupling in *cis*-[PdR₂(PR'₃)₂] complexes can occur directly, or on tetracoordinated intermediates *cis*-[PdR₂(PR'₃)L] formed upon addition of an additive L, or on tricoordinated intermediate [PdR₂(PR'₃)] formed by phosphine dissociation. The size and nature of the R group and the phosphine, as well as the coordinating features of L, have a determinant influence on the coupling mechanism. The ancillary ligands used in catalysis can be critical to the feasibility of a catalytic cycle.

In difficult couplings, the addition of olefins with electron-withdrawing substituents as coupling promoters can be decisive for the success of the coupling, as the formation of a coupling

(39) See also refs 23 and 29.

(40) Calculated free energy values are $\Delta G = -6.4$ kcal mol for R = Ph versus 5.5 kcal mol for R = Me. The trend in computed free energies thus confirms the easier dissociation for PPh₃. The absolute free energy values should not be taken, however, as quantitatively correct. In fact, if these values were quantitatively correct, the complex with PPh₃ should be observed as fully dissociated. Even if dissociation was only 1%, the dissociated species should be detected (by NMR at 250 K). This is not the case, suggesting that *cis*-[PdMe₂(PPh₃)₂]:[PdMe₂(PPh₃)] $\geq 100:1$, wherefrom $\Delta G_{\text{eq,dis.}}$ (250 K) ≥ 2.3 kcal mol for R = Ph. It is well known that entropic contributions for bimolecular processes are overestimated in this type of calculations.

(41) Guille, A.; Stille, J. K. *J. Am. Chem. Soc.* **1980**, *102*, 4933–4941.

(42) There are two reasons for this: (a) Assuming that the order of activation energy found for PMe₃ complexes is maintained for PPh₃ complexes, coupling is faster in the tricoordinated intermediate formed by PPh₃ dissociation than in the tetracoordinated complex formed with a common olefin (roughly speaking, ligands in entries 1–4 of Table 2). (b) In energetically limiting cases, it would help to lack of effect that the amount of a putative tetracoordinated intermediate with coordinated olefin is probably insignificant.

(43) (a) Williams, D. B. G.; Shaw, M. L. *Tetrahedron* **2007**, *63*, 1624–1629. (b) Luo, X.; Zhang, H.; Duan, H.; Liu, Q.; Zhu, L.; Zhang, T.; Lei, A. *Org. Lett.* **2007**, *9*, 4571–4574.

intermediate cis -[PdMe₂(PR₃)(acceptor olefin)] can reduce the coupling barrier up to 15 kcal/mol (higher concentration of this kind of active intermediate can be favored using phosphine-olefin chelating ligands). It should be noted, however, that olefins with electron-withdrawing substituents disfavor the subsequent oxidative addition and could render this step rate determining in the cycle.⁴⁴ Hence, a tradeoff between the two effects of acceptor olefins should be reached in each case.

Bulkier phosphines help to access to lower energy dissociative couplings. Because coupling on a tricoordinated complex has lower activation energy than most couplings on a tetracoordinated complex, the use of bulky phosphines that facilitate ligand dissociation favors a faster coupling. Furthermore, when the coupling takes place on tricoordinated intermediates, the more difficult alkyl–alkyl couplings come closer in activation energy to the easier phenyl–phenyl or vinyl–vinyl couplings. Hence, the positive effect of bulky ancillary ligands is particularly important for the case of alkyl–alkyl coupling.

Interestingly, the calculations suggest and the experiment shows that in cases where a low coupling barrier is operating via a tricoordinated intermediate (e.g., with bulky phosphines), the addition of small electron-deficient olefins able to coordinate can still help very noticeably to further accelerate the coupling rate (e.g., 7.3 kcal/mol reduction of the coupling barrier is observed in Table 2 comparing entries 8 and 7), forming a cis -[PdR₂(bulky phosphine)(acceptor olefin)] intermediate with even lower activation energy. In summary, this study explains the effect of potentially coordinating additives on the reductive elimination and opens the path for the experimental design of more efficient catalytic systems.

Experimental Section

Kinetic Study of the Reductive Elimination. The kinetic experiments were monitored by ¹H NMR at 400 MHz. NMR tubes (5 mm) were charged with the corresponding olefin. Next, the tubes

were cooled at –78 °C, and a solution of cis -[PdMe₂(PPh₃)₂]⁴⁵ (**4**) in acetone-*d*₆ was added (0.7 mL). The tubes were placed into a thermostated probe. Concentration–time data were then acquired from ¹H integration of signals of **4**. The experimental data are collected in Tables 3 and 4. The exact temperature was calibrated with an ethylene glycol standard for Table 3, and with a methanol standard for Table 4.

Acknowledgment. We thank the Spanish Ministerio de Educación y Ciencia (INTECAT Consolider Ingenio-2010 (CSD2006-0003), and Consolider Ingenio 2010 (CSD2007-00006); SAF07-63880, FEDER; CTQ2005-09000-CO2-01; CTQ2005-09000-CO2-02; CTQ2007-67411/BQU; CTQ2008-06647-CO2-01/BQU; “Juan de la Cierva” contract to A.A.C.B.; studentship to M.H.P.-T.); the Xunta de Galicia (Parga Pondal Contract to M.P.-R.); the Catalan DURSI through project 2005SGR00715; the Junta de Castilla y León (Projects VA044A07 and GR169); the UAB for a PIF studentship to M.G.-M.; and the ICIQ foundation for financial support. We also thank CESGA and CESA for generous allocation of computational resources.

Supporting Information Available: Computational methods. Complete computational data and discussion for the complexes with R = Me, Ph, and vinyl and L = PMe₃, MeCN, empty, CH₂CH₂, ma. Computational data for the complexes with R = Me and L = *trans*-2-butene, 2,5-dihydrofuran, 3,5-dimethylcyclopent-1-ene, *trans*-1,2-dicyanoethylene, *p*-benzoquinone. Data for the ligand dissociation from cis -[PdMe₂(PPh₃)₂] and cis -[PdMe₂(PMe₃)L], and for the olefin rotation in cis -[PdMe₂(PMe₃)(H₂C=CH₂)]. This material is available free of charge via the Internet at <http://pubs.acs.org>.

JA808036J

(44) Fairlamb, I. J. S.; Kapdi, A. R.; Lee, A. F.; McGlacken, G. P.; Weissburger, F.; de Vries, A. H. M.; Schmieder-van de Vondervoort, L. *Chem.-Eur. J.* **2006**, *12*, 8750–8761, and references therein.

(45) Byers, P. K.; Canty, A. J.; Jin, H.; Kruis, D.; Markies, B. A.; Boersma, J.; van Koten, G. *Inorg. Synth.* **1998**, *32*, 170.